ESC European Society of Cardiology

European Heart Journal - Cardiovascular Imaging (2017) **18**, 1128–1137
doi:10.1093/ehjci/jex097

Left atrial structure and function in cardiac amyloidosis

Kotaro Nochioka[1,2], Candida Cristina Quarta[3,4†], Brian Claggett[1], Gabriela Querejeta Roca[1], Claudio Rapezzi[4], Rodney H. Falk[5], and Scott D. Solomon[1*]

[1]Cardiovascular Division, Brigham and Women's Hospital, Harvard Medical School, 75 Francis Street Boston, MA 02115, USA; [2]Department of Cardiovascular Medicine, Tohoku University Graduate School of Medicine, Clinical Research, Innovation and Education Center, Tohoku University Hospital, Seiryo-machi 1-1 Aobaku Sendai, Miyagi 980-8574, Japan; [3]Division of Medicine, National Amyloidosis Centre UCL, Royal Free Hospital, Rowland Hill Street, London NW3 2PF, UK; [4]Cardiology, Department of Experimental Diagnostic and Specialty Medicine, Alma Mater Studiorum University of Bolonga, PAD 21,Policlinico S.Orsola-Malpighi, via Massarenti 9, 40138 Bologna, Italy; and [5]Department of Cardiology, Harvard Vanguard Medical Associates, Brigham and Women's Hospital Cardiac Amyloidosis Program, Harvard Medical School, 75 Francis Street Boston, MA 02115, USA

Received 20 January 2017; editorial decision 28 March 2017; accepted 27 April 2017; online publish-ahead-of-print 16 June 2017

Aims Although cardiac amyloidosis (CA) is characterized by significant left atrial (LA) dilatation, the characteristics of LA function remain to be fully investigated.

Methods and results We assessed LA function by speckle-tracking echocardiography in 124 patients with CA and sinus rhythm: 68 with light chain (AL), 29 with mutant (ATTRm), 27 with wild-type (ATTRwt) transthyretin amyloidosis. Conventional and strain-derived parameters, including LA peak longitudinal strain (LS) and strain rate (peak LSR: reservoir function; early LSR: conduit function; late LSR: active function), were assessed compared between CA patients and 20 healthy controls of similar age and gender.

All LA function phases, including LA longitudinal strain, peak LSR, early and late LSR were significantly impaired in CA compared to healthy controls after adjusting for LA size, LV ejection fraction and LV filling pressures (*E*/*E*') (all $P < 0.05$). Peak LA LS was moderately correlated with LV global LS ($R = -0.60$, $P < 0.001$); late LSR was correlated with A wave at the level of LV inflow ($R = -0.69$, $P < 0.001$). Among the different CA subtypes, peak LS and LA active emptying fraction were worse in ATTRwt than AL and ATTRm [$P < 0.05$ after adjustment for age, sex, body mass index, systolic blood pressure, heart rate, LA volume index, severity of mitral regurgitation, left ejection fraction, and left ventricular end-diastolic pressure (*E*/*E*')].

Conclusion In CA, LA function was severely impaired and highly correlated with LV deformation. Differences in LA function between amyloid subtypes suggest that amyloid aetiology plays a role in the pathophysiology of cardiac dysfunction in CA.

Keywords amyloid • cardiomyopathy • left atrial function • echocardiography • 2D speckle tracking

Introduction

Cardiac amyloidosis (CA) is caused by intramyocardial amyloid infiltration[1,2] due to one of the several aetiologies, including: immunoglobulin light chains (AL) amyloidosis, in which a clonal plasma cell dyscrasia produces the immunoglobulin light chains responsible of the amyloid deposits; hereditary transthyretin (TTR) amyloidosis (ATTRm), which can be caused by over 100 point mutations in the *TTR* gene, and non-hereditary (i.e. wild-type) TTR amyloidosis (ATTRwt), which mainly affects the heart of elderly men.[1,2]

Amyloid can virtually infiltrate all cardiac chambers. Most studies have focused on the consequences of amyloid infiltration throughout the left ventricle (LV), which include a progressive increase of wall thickness and LV stiffness.[1,3,4] Left atrial (LA) or bi-atrial enlargement

* Corresponding author. Tel: +1 857 307 1960; Fax: +1 857 307 1944. E-mail: ssolomon@rics.bwh.harvard.edu

† Co-first author.

is a common finding in CA.[5] However, LA enlargement is an anatomical measurement and does not necessarily reflect its function. Although LA size has been reported to be a poor prognostic indicator in CA patients,[6] a comprehensive and quantitative characterization of LA function and its implications in CA is lacking.

2D myocardial deformation imaging is a robust and sensitive echocardiographic technique for the quantitative assessment of LA function[7] and has proven to play an adjunctive role in the diagnosis and prognostic stratification of CA.

We used 2D-derived speckle-tracking imaging to characterize LA function in CA and to determine whether the progressive reduction of LA contribution to LV filling is secondary to the restrictive LV physiology, intrinsic LA dysfunction due to direct amyloid infiltration, or a combination of both. We also compared the profiles of the different CA subtypes to investigate whether any observed differences in LA structure and function might account for the reported markedly different prognoses, (median survival ~6 months in untreated AL CA vs. 6 years in ATTRwt.[8]

Methods

Setting and study design

We conducted a multicentre retrospective study of patients with aetiologically defined CA from two large international amyloidosis centres, the Brigham and Women's Hospital (BWH, Boston) and the S.Orsola-Malpighi Hospital (Bologna). All consecutive patients diagnosed with CA at the Brigham and Women's Hospital (Boston) from 2006 to 2012 ($n = 110$), or at the S.Orsola-Malpighi Hospital (Bologna) from 2009 to 2012 ($n = 62$) as previously reported[4] were reviewed. Patients were included in the present analysis if sinus rhythm was documented at the time of their presentation at either centre. We compared their baseline clinical profiles and echocardiographic parameters, with particular focus on LA structure and function, with those of 20 healthy controls retrospectively identified from the medical records of the BWH. Furthermore, we compared the LA indices among the different aetiologic subtypes. At the Bologna centre, all patients provided informed consent for anonymous publication of scientific data. At the Boston centre, the collection of anonymized medical records was approved by the institutional review board.

Definitions of cardiac amyloidosis, aetiological subtype, and control

Definition of systemic amyloidosis, including aetiological diagnosis of AL, ATTRm, and ATTRwt amyloidosis, and CA have been previously reported.[4] Briefly, diagnosis of systemic amyloidosis was defined by histological documentation of Congo-red staining and apple-green birefringence under cross-polarized light in at least one involved organ.[9]

Cardiac involvement was defined as an echocardiographic end-diastolic LV wall thickness greater than 1.2 cm (in the absence of any other plausible causes of LV hypertrophy).[1,2,10] Other echocardiographic signs suggesting CA (in addition to increased LV wall thickness) included: granular sparkling appearance of the myocardium, increased thickness of atrioventricular valves, right ventricular free wall, or interatrial septum, and pericardial effusion. In selected cases with equivocal echocardiographic findings who did not undergo an endomyocardial biopsy, cardiac magnetic resonance and nuclear imaging, including ^{99m}Tc-labelled 3,3-diphosphono-1,2-propanodicarboxylic acid (DPD, available in Europe) and ^{99m}Tc-labelled pyrophosphate (PYP, available in the USA) were performed to confirm the presence and nature of intramyocardial amyloid deposits.[11,12]

Distinction between AL and TTR-related amyloidosis was based on genotyping and/or immunohistochemistry or mass spectrometry.[1,9] AL was defined by the presence of monoclonal plasma cell dyscrasia with serum electrophoresis, serum or urine immunofixation, and abnormal serum free light chain assay, in the absence of any TTR mutation at DNA analysis.[13,14] Diagnosis of familial ATTRm was defined by a documented TTR mutation with DNA analysis following procedures described elsewhere.[15] ATTRwt was defined by positive immunohistochemistry for TTR in the absence of any TTR mutation at DNA analysis.[16] In equivocal cases, biopsy specimens underwent proteomics evaluation.[17]

A group of 20 healthy controls were retrospectively identified from the medical records of the BWH. The search strategy targeted patients aged 55 years or older, who had an echocardiogram and no International Classification of Diseases 9th Revision (ICD-9) code in their record for any of the following conditions: hypertension, ischaemic heart disease, cardiac arrhythmia, dyslipidaemia, chronic obstructive lung disease, diabetes mellitus, cerebrovascular disease, arterial vascular disease, and cancer. This group was further selected to have normal LV ejection fraction (LVEF), no LV regional motion abnormalities, normally sized cardiac chambers, no significant valvular disease, and suitable echocardiogram image quality. Controls had a similar age and gender distribution to the CA group.

Echocardiographic methods

Echocardiograms were performed at both centres using commercially available ultrasound systems (iE33, Philips Medical Systems and Vivid 7, GE Medical Systems, Milwaukee, WI). Images were acquired in DICOM format using a frame rate of 50–70 fps. Analysis of the echocardiographic images (both conventional and speckle tracking-derived measurements) was conducted at the cardiac imaging core laboratory of the Brigham and Women's Hospital, blinded to clinical information, as previously described.[4] A minimum of three cardiac cycles were recorded for each image and measurement were averaged accordingly.

Standard echocardiographic and Doppler parameters were analysed using an offline analysis workstation. All measurements were made in accordance with the recommendations of the American Society of Echocardiography (ASE).[18–20]

Because dedicated software for LA strain analysis has not yet been released, we used 2D speckle tracking vendor-independent software with algorithms designed for LV analysis (TomTec Imaging Systems, Germany) to study LA deformation.

If more than two segments in LA and LV could not be tracked or there was a lack of a full cardiac cycle, missing views, non-DICOM images, significant foreshortening of the cavities, or pulmonary vein drop out for the images focused on the LA, the measurements were considered unreliable and the patient was excluded from the analysis. Speckles were tracked frame by frame throughout the LA and LV myocardium over the course of one cardiac cycle; basal, mid, and apical regions of interest were then created. Semi-quantitative segment tracking was carefully inspected. The LA and LV endocardial borders were traced at the end-diastolic frame. End-diastole was defined by the QRS complex or as the frame after mitral valve closure.

For LV deformation, global longitudinal strain (GLS) was calculated as the average LV longitudinal strain across the 12 segments obtained using apical 4- and 2-chamber views as previously described.[4]

For LA speckle tracking analysis, LA phasic function was measured using volumes and strain indices calculated as the average of the 12 segments obtained using apical 4- and 2-chamber views. LA time-volume curves were generated by calculating LA volume at each phase of the cardiac cycle (LA maximal, LA pre-A, and LA minimum volumes) using the Simpson method. From these LA volumes, LA phasic function was estimated as (*Figure 1A*):

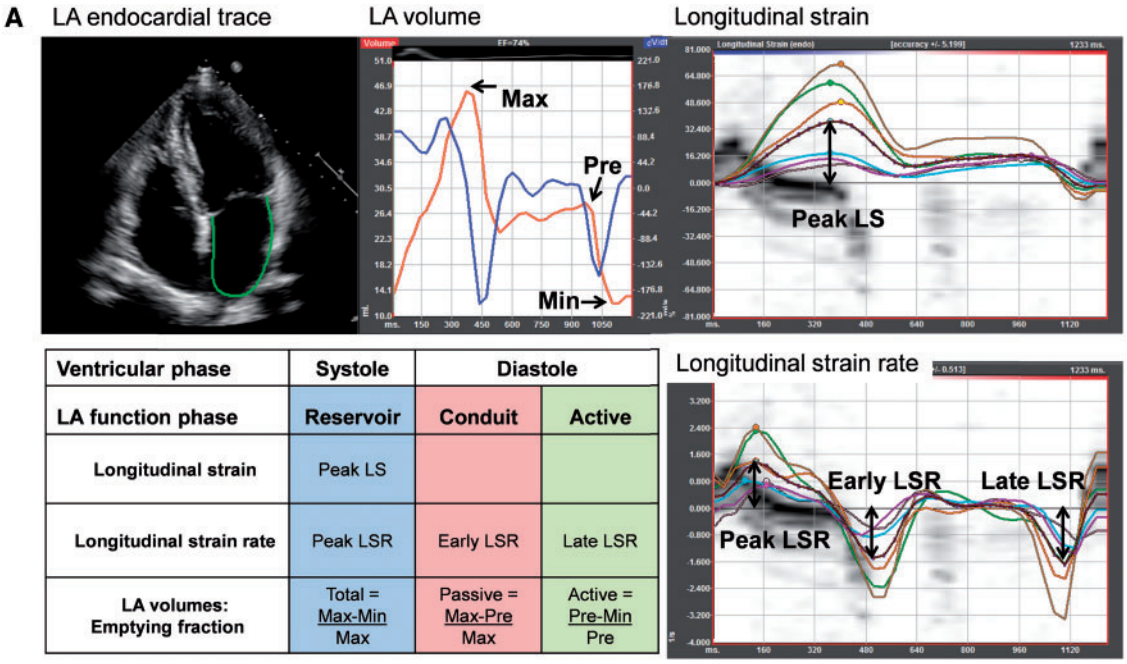

Ventricular phase	Systole	Diastole	
LA function phase	Reservoir	Conduit	Active
Longitudinal strain	Peak LS		
Longitudinal strain rate	Peak LSR	Early LSR	Late LSR
LA volumes: Emptying fraction	Total = Max-Min / Max	Passive = Max-Pre / Max	Active = Pre-Min / Pre

Figure 1 (*A*) Representative examples of left atrial (LA) measurements in a healthy control case. LA maximal volume (Max), LA pre emptying volume (Pre), LA minimal volume (Min), longitudinal strain (LS), and longitudinal strain rate (LSR). (*B*) Representative examples of LA measurements in a patient with advanced cardiac amyloidosis with enlarged LA and lower LA peak LS, peak LSR, early LSR, and late LSR.

- LA emptying fraction (reservoir function) = ([LA maximum volume - LA minimal volume] / LA maximum volume) × 100
- LA passive emptying fraction (conduit function) = ([LA maximum volume - LA pre-A volume] / LA maximum volume) × 100
- LA active emptying fraction (pump function) = ([LA pre-A volume - LA minimal volume]/LA pre-A volume] × 100.

From the LA strain analysis, LA reservoir function was estimated using peak strain during ventricular systole (systolic or peak LA strain), which represents the LA filling during LV systole. Because the LA expands during ventricular systole, peak LA strain is a positive strain value. LA conduit function was estimated using the early peak strain rate (SR) during LV diastole (LA passive SR), while LA pump function was estimated using late peak SR during LV diastole (LA active SR). (*Figure 1A and B*).[21–23]

All measurements were performed by a single investigator blinded to clinical status. Intraobserver variability for LA LS and LSR was assessed by measuring three times in the whole sample. The coefficients of variation

for LA measures were as follows: LA LS 10.9%, peak LSR 13.2%, early LSR 13.6%, and late LSR 23.5%.

Follow-up

In both centres, follow-up visits were planned for every 6 months (or more frequently if clinically appropriate). Follow-up was closed in May 2013; for patients who had not attended a visit in the last 6 months, vital status was ascertained by telephone and/or by contacting referring physicians. However, of 124 patients, 11 patients had missing information on death and were excluded from the analysis.

During a median follow-up of 24.4 [17–33] months, we observed 34 (30%) deaths (27 among AL patients, 3 among ATTRm patients, and 4 among ATTRwt patients), with a death rate of 1.8/100 person years among AL patients, 0.3/100 person years among ATTRm patients, and 0.6/100 person years among ATTRwt patients (see Supplementary data online, *Figure S1*).

Statistical analysis

Summary statistics were expressed as mean ± standard deviation (SD), median (interquartile range) or numbers (percentages). Comparisons between CA patients and healthy controls were performed using Student's *t*-test for continuous normally distributed variables, Mann–Whitney test for continuous non-normally distributed variables, and Fisher exact test for categorical variables. Pearson's correlation coefficient was used to evaluate the correlation between LA function and age, systolic blood pressure, heart rate, LV function, LV structure, and LA size.

In a subgroup analysis, we divided the CA group into severely enlarged (left atrial volume index (LAVI) ≥ 48 mL/m^2) and not severely enlarged LA (LAVI < 48 mL/m^2) according to ASE guidelines.[18,19]

When comparing the profile of the three different CA subtypes, continuous variables were tested using one-way analysis of variance or Kruskal–Wallis test in case of normally and not normally distributed variables, respectively. Additional comparisons between CA subtypes were performed using multivariable linear regression to adjust for variables that may influence LA size or function, including age, sex, BMI, systolic blood pressure, heart rate, LA volume index to body surface area, severity of mitral regurgitation, LVEF and LV end-diastolic pressure as measured by mitral inflow to mitral relaxation velocity ratio (*E/E'*).

Analyses were conducted using STATA 13 SE (Stata Corporation, College Station, TX). All tests were two-sided and a *P*-value < 0.05 was considered statistically significant.

Results

Study population and baseline characteristics

Of the 172 patients diagnosed with CA during the study period, 124 (72%) were in sinus rhythm at the time of echocardiography and were included in the present analysis (AL, *n* = 68; ATTRm, *n* = 29; ATTRwt, *n* = 27). Among patients with ATTRm, TTR variants were distributed as follows: Ile68Leu (*n* = 8), Glu89Gln (*n* = 6), Val122Ile (*n* = 4), Thr60Ala (*n* = 4), Thr49Ala (*n* = 2), Val30Met (*n* = 1), Arg34Thr (*n* = 1), Glu54Gln (*n* = 1), Gly47Ala (*n* = 1), Thr59Lys (*n* = 1).

Compared to patients in sinus rhythm, those without were older, more frequently male, with a higher prevalence of ATTRm, more advanced heart failure symptoms and more frequent history of heart failure hospitalizations as well as beta blocker and diuretic usage (see Supplementary data online, *Table S1*).

Tables 1 and 2 summarize the demographic, clinical and echocardiographic findings in the overall CA population (*n* = 124) compared to healthy controls (*n* = 20) and according to the specific aetiology of CA, respectively. As expected, all echocardiographic measures, including interventricular septum, posterior wall, LV end-diastolic volume, ejection fraction, and GLS, E/E', as well as LA volume and width, were abnormal in CA patients (*Table 1*).

As anticipated, ATTRwt patients were more likely to be elderly males with longer disease duration and a higher degree of both morphological and functional echocardiographic impairment, including thicker cardiac walls and worse contractility and longitudinal systolic

Table 1 Demographic, clinical, and echocardiographic characteristics in healthy controls vs. cardiac amyloidosis

	Healthy controls *n* = 20	CA *n* = 124	*P*-value
Age, years	66.5 ± 5.0	64.1 ± 11.9	0.37
Male sex, *n* (%)	13 (65.0)	86 (69.4)	0.70
Aetiology, *n* (%)			
AL		68 (54.8)	
ATTRm		29 (23.4)	
ATTRwt		27 (21.8)	
Systolic blood pressure, mmHg	125 ± 15	119 ± 20	0.27
Diastolic blood pressure, mmHg	72 ± 13	72 ± 10	0.91
Heart rate, bpm	74 ± 19	76 ± 14	0.55
BMI, kg/m^2	24.2 ± 3.8	25.2 ± 4.3	0.33
Echocardiography			
LVEDD, cm	4.4 ± 0.6	4.3 ± 0.6	0.44
IVS, cm	1.0 ± 0.2	1.6 ± 0.3	<0.001
PW, cm	0.9 ± 0.1	1.5 ± 0.2	<0.001
LVEDV/BSA, mL/m^2	53.3 ± 11.8	45.7 ± 11.5	0.017
LVESV/BSA, mL/m^2	22.3 ± 8.2	20.4 ± 7.9	0.38
LV mass index (BSA), g/m^2	81.9 ± 19.0	147.1 ± 42.1	<0.001
LV ejection fraction, %	59.4 ± 3.5	56.0 ± 11.0	0.19
GLS, %	-19.9 ± 2.5	-13.0 ± 4.2	<0.001
E wave, m/s			
A wave, m/s	0.7 ± 0.2	0.6 ± 0.3	0.023
EA ratio	1.0 ± 0.2	1.8 ± 1.0	<0.001
E' (lateral), cm/s	9.5 ± 2.1	6.1 ± 2.2	<0.001
E/E' (lateral)	7.4 ± 2.0	15.1 ± 7.6	<0.001
A' (lateral), cm/s	10.66 ± 2.63	5.91 ± 2.98	<0.001
S' (lateral), cm/s	8.39 ± 1.71	5.72 ± 2.15	<0.001
LA structure			
LA volume (BSA) mL/m^2	20.8 ± 4.2	37.7 ± 13.0	<0.001
LA width, cm	3.4 ± 0.4	4.4 ± 0.6	<0.001

BMI, body-mass index; LVEDD, left ventricular end-diastolic dimension; IVS, interventricular septum; PW, posterior wall; LVEDV, left ventricular end-diastolic volume; LVESV, left ventricular end-systolic volume; BSA, body surface area; GLS, global longitudinal strain; E/A, early to late mitral inflow velocity ratio; E', lateral mitral early relaxation velocity; A', lateral mitral late relaxation velocity; S', lateral mitral systolic velocity; E/E', mitral inflow to mitral relaxation velocity ratio; CA, cardiac amyloidosis.

Table 2 Demographic, clinical, and echocardiographic characteristics according to the aetiological subtype of cardiac amyloidosis

Total *n* = 124	AL *n* = 68	ATTRm *n* = 29	ATTRwt *n* = 27	*P*-value (AL vs. ATTRm)	*P*-value (AL vs. ATTRwt)
Age, years	62.1 ± 10.7	59.1 ± 13.1	74.4 ± 6.5*	0.23	<0.001
Male sex, *n* (%)	43 (63.2)	20 (69.0)	23 (85.2)	0.59	0.036
NYHA class III ot IV, *n* (%)	15 (22.1)	7 (24.1)	6 (22.2)	0.82	0.99
Systolic blood pressure, mmHg	113.4 ± 17.2	126.0 ± 20.3	126.8 ± 21.5	0.004	0.004
Diastolic blood pressure, mmHg	69.3 ± 9.4	76.0 ± 11.5	73.7 ± 9.9	0.006	0.06
Heartrate, bpm	78.2 ± 13.9	76.1 ± 13.5	70.4 ± 15.6	0.5	0.02
BMI, kg/m	24.8 ± 4.2	26.1 ± 4.4	25.0 ± 4.2	0.17	0.8
Previous history of HF hospitalization, *n* (%)	41 (60.3)	11 (37.9)	20 (74.1)*	0.043	0.21
Disease duration,[a] months	8.6 [3.5, 15.0]	15.4 [5.2, 40.0]	24.4 [6.0, 37.0]	0.021	0.028
Kidney involvement[b], *n* (%)	30 (48.4)	0	1 (3.8)	<0.001	<0.001
eGFR, mL/min/1.73 m^2	64.6 ± 27.7	73.0 ± 26.9	56.6 ± 17.0*	0.24	0.22
NT-proBNP, median [IQR]	3169 [1321, 12517]	2093 [1111, 3447]	2365 [1255, 4175]	0.1	0.28
Beta blocker, *n* (%)	18 (27.7)	11 (39.3)	9 (34.6)	0.27	0.51
Ca blocker, *n* (%)	3 (4.6)	2 (7.1)	0	0.62	0.27
Amiodarone, *n* (%)	2 (3.0)	1 (3.6)	5 (19.2)	0.89	0.008
Diuretics, *n* (%)	38 (57.6)	18 (64.3)	21 (80.8)	0.54	0.037
RAS-I, *n* (%)	12 (18.2)	6 (21.4)	6 (23.1)	0.71	0.59
Echocardiography					
LVEDD, cm	4.2 ± 0.5	4.4 ± 0.6	4.3 ± 0.6	0.018	0.2
IVS, cm	1.5 ± 0.2	1.5 ± 0.3	1.7 ± 0.3*	0.9	<0.001
PW, cm	1.4 ± 0.2	1.4 ± 0.2	1.6 ± 0.2*	0.35	0.002
LV mass/BSA, g/m^2	138.5 ± 36.5	148.0 ± 44.8	167.8 ± 46.1	0.28	0.002
LVEDV/BSA, mL/m^2	44.5 ± 10.7	48.1 ± 11.4	46.1 ± 13.6	0.14	0.55
LVESV/BSA, mL/m^2	19.1 ± 6.6	21.3 ± 9.4	22.7 ± 8.9	0.19	0.033
LV ejection fraction, %	57.5 ± 9.4	56.9 ± 12.6	51.3 ± 11.7	0.79	0.008
GLS, %	-12.6 ± 4.0	-15.2 ± 4.1	-11.7 ± 3.9*	0.006	0.32
E wave, m/s	0.8 ± 0.2	0.8 ± 0.2	0.7 ± 0.2*	0.74	0.036
A wave, m/s	0.6 ± 0.3	0.7 ± 0.3	0.4 ± 0.2*	0.21	0.011
E/A	1.8 ± 0.9	1.6 ± 0.9	2.2 ± 1.1*	0.35	0.07
E' (lateral), cm/s	5.9 ± 2.1	6.8 ± 2.9	5.8 ± 1.2	0.13	0.93
E/*E*' (lateral)	16.3 ± 8.8	14.0 ± 6.4	12.9 ± 4.5	0.24	0.1
A' (lateral), cm/s	6.1 ± 2.9	6.68 ± 3.40	4.1 ± 1.8*	0.45	0.016
S' (lateral), cm/s	6.0 ± 2.2	5.92 ± 2.34	4.7 ± 1.3*	0.91	0.017
LA volume/BSA, mL/m^2	35.6 ± 12.4	36.7 ± 12.2	44.0 ± 13.9*	0.67	0.006
LA width, cm	4.3 ± 0.5	4.2 ± 0.6	4.8 ± 0.5	0.75	<0.001
Mitral regurgitation, *n* (%)				0.16	0.16
I	26 (38.8)	6 (21.4)	8 (29.6)		
II	25 (37.3)	9 (32.1)	12 (44.4)		
III	7 (10.4)	1 (3.6)	5 (18.5)		
IV	4 (6.0)	0	0		

NYHA, New York Heart Association; eGFR, glomerular filtration rate; BMI, body mass index; LVEDD, left ventricular end-diastolic dimension; IVS, interventricular septum; PW, posterior wall; LVEDV, left ventricular end-diastolic volume; LVESV, left ventricular end-systolic volume; BSA, body surface area; GLS, global longitudinal strain; E/A, early to late mitral inflow velocity ratio; E', lateral mitral early relaxation velocity; A', lateral mitral late relaxation velocity; S', lateral mitral systolic velocity; E/E', mitral inflow to mitral relaxation velocity ratio; IQR, interquartile range; HF, heart failure.

[a]Disease duration was calculated as the time interval between the onset of symptoms and the final diagnosis of the amyloid disease. The onset of symptoms was derived by patients' self-report of striking changes in their clinical condition in the past weeks/months/years that were judged to be compatible with manifestations of the disease.

[b]Kidney involvement was defined as the presence of 24-hour urine protein excretion ≥0.5 g/d, and renal insufficiency was defined as glomerular filtration rate <60 mL/min.

*Significant (*P*-value < 0.05) for ATTRm vs. ATTRwt.

function (*Table 2*). No statistical differences were observed among the three aetiologies of CA in NT-proBNP levels or glomerular filtration rate.

LA structure and function

Table 3 summarizes the LA phasic function in CA patients vs. healthy controls. Compared to healthy controls, CA patients showed worse strain-derived LA reservoir, conduit and active function, including peak LS, peak LSR, early LSR, and late LSR, even after adjusting for LA volume indexed to body surface area (LAVI), left ventricular ejection fraction, and left ventricular end-diastolic pressure (E/E') (*Table 3*).

Table 3 LA reservoir, conduit and active function: patients with cardiac amyloidosis vs. healthy controls

LA function	Healthy Controls *n* = 20	CA *n* = 124	Unadjusted *P*-value
Reservoir function			
Peak LS, %	40.6 ± 6.2	18.8 ± 11.6	<0.001*
Peak LSR, S^{-1}	1.60 ± 0.46	0.84 ± 0.47	<0.001*
Total emptying fraction, %	61.0 ± 11.0	45.1 ± 16.7	<0.001*
Conduit function			
Early LSR, S^{-1}	-1.38 ± 0.43	-0.71 ± 0.37	<0.001*
Passive emptying fraction, %	30.7 ± 11.8	25.7 ± 11.3	0.1
Active function			
Late LSR, S^{-1}	-1.48 ± 0.43	-0.84 ± 0.76	0.001*
Active emptying fraction, %	42.3 ± 11.6	28.6 ± 16.6	0.001*

Data are shown as mean ± SD.
LS, longitudinal strain; LSR, longitudinal strain rate.
*Significant (*P*-value <0.05) after adjustment for LA volume index (LAVI), left ventricular ejection fraction, and left ventricular end-diastolic pressure (E/E').

The unadjusted comparison between AL, ATTRm, and ATTRwt (*Table 4*) did not show any significant differences in LA phasic (reservoir, conduit and active) functions, although ATTRwt showed lower peak LS, peak LSR, early LSR, late LSR, and active emptying fraction. LA peak LS was frequently impaired in all aetiologies, being abnormal (i.e. under -1.96 SD from the mean value in the control group) in 81%, 74%, and 91% of AL, ATTRm, and ATTRwt patients, respectively. ATTRwt aetiology was associated with significantly lower LA peak LS and LA active emptying fraction when adjusting for age, gender, body mass index, systolic blood pressure, heart rate, LAVI, severity of mitral regurgitation, LV ejection fraction, and LV end-diastolic pressure (*E/E'*) (*Table 4*).

When stratifying CA patients by the severity of LA enlargement (LAVI cut-off = 48 mL/m^2),[18,19] those with LAVI ≥ 48 mL/m^2 showed worse LA reservoir and active function compared to both healthy controls and CA patients with LAVI < 48 mL/m^2 (*Figure 2*). However, when considering LA conduit function, only LSR was worse in CA patients with severely dilated LA.

Correlation between LA strain measures and other clinical and echocardiographic findings

Overall, in CA patients, LA reservoir, conduit and pump functions were correlated with LV mass index, parameters of LV function and LA size (*Table 5*). LV GLS was correlated with LA peak LS (Pearson $R = -0.60$, $P < 0.0001$), peak LSR ($R = -0.54$, $P < 0.0001$) and late LSR ($R = -0.54$, $P < 0.0001$); a weak correlation between LV GLS and early LSR ($R = 0.30$, $P = 0.0020$) was also observed. Notably, Late LSR also showed a strong negative correlation with A wave measured at the mitral inflow level ($R = -0.69$, $P < 0.0001$).

Table 4 LA reservoir, conduit and active function: within each aetiological subgroup

LA function	AL *n* = 68	ATTRm *n* = 29	ATTRwt *n* = 27	Unadjusted *P*-value
Reservoir function				
Peak LS, %	19.3 ± 11.4	20.1 ± 13.9	16.1 ± 9.1**	0.47
Peak LSR, S^{-1}	0.89 ± 0.48	0.88 ± 0.54	0.65 ± 0.29	0.12
Total emptying fraction, %	45.9 ± 17.8	45.7 ± 16.8	42.6 ± 14.0	0.73
Conduit function				
Early LSR, S^{-1}	-0.71 ± 0.34	-0.81 ± 0.53	-0.59 ± 0.21	0.13
Passive emptying fraction, %	25.7 ± 11.7	23.6 ± 11.3	27.8 ± 10.3	0.16
Active function				
Late LSR, S^{-1}	-0.88 ± 0.76	-0.95 ± 0.91	-0.61 ± 0.57	0.28
Active emptying fraction, %	29.5 ± 17.0	31.8 ± 16.9	22.3 ± 14.1***	0.16

Data are shown as mean ± SD.
LS, longitudinal strain; LSR, longitudinal strain rate.
*Significant (*P*-value < 0.05) among groups. after adjusting for age, sex, body mass index, systolic blood pressure, heart rate, left atrial volume indexed to body surface area, severity of mitral regurgitation, left ventricular ejection fraction and left ventricular end-diastolic pressure (E/E').
**Significant (*P*-value < 0.05) for ATTRwt vs. AL and ATTRm after adjusting for age, sex, body mass index, systolic blood pressure, heart rate, left atrial volume indexed to body surface area, severity of mitral regurgitation, left ventricular ejection fraction and left ventricular end-diastolic pressure (E/E').

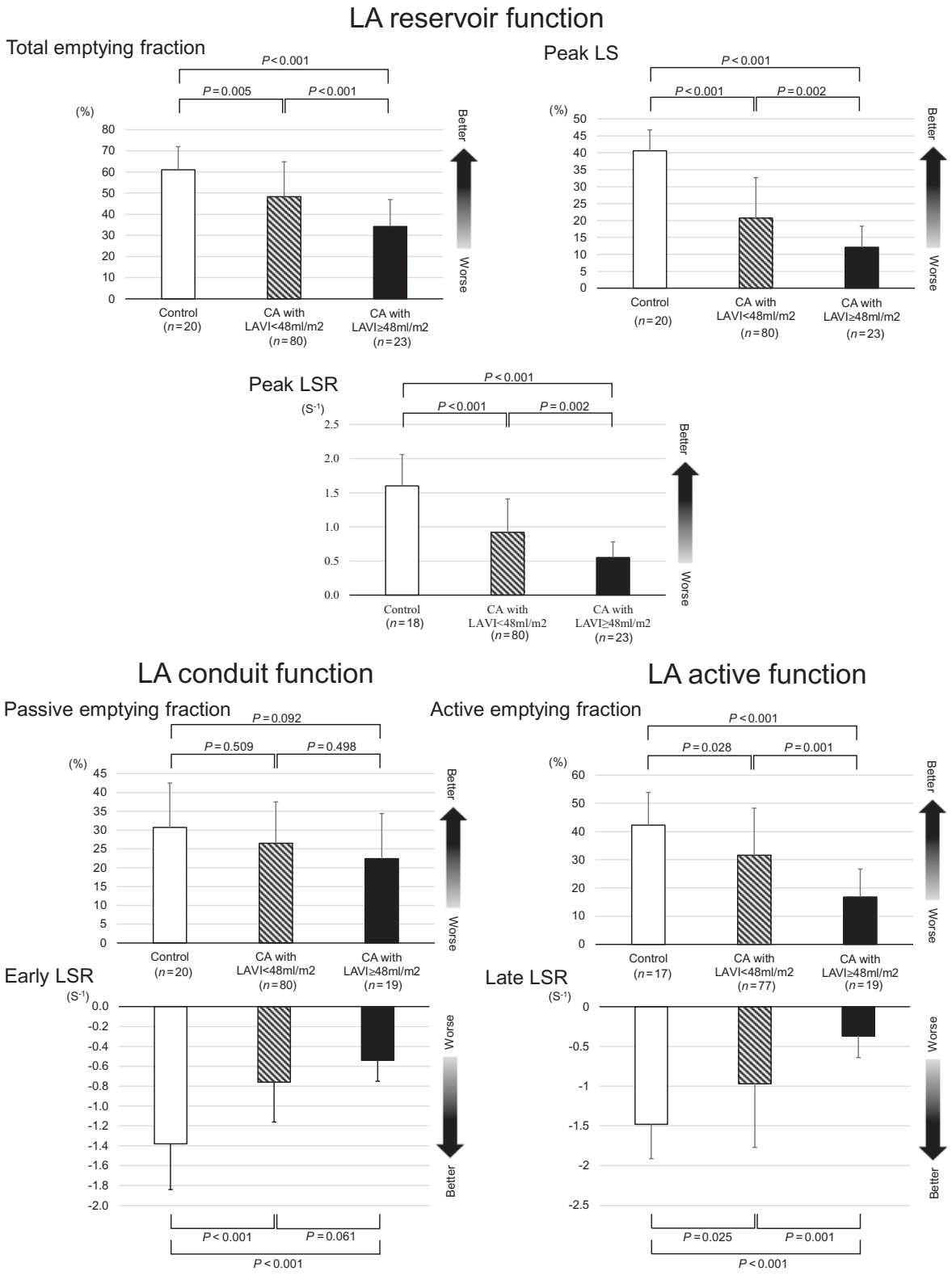

Figure 2 Comparison of left atrial (LA) function (reservoir, conduit and pump functions) in healthy controls and cardiac amyloidosis (CA) patients with LA volume index (LAVI) < 48 mL/m^2 and CA patients with LAVI > 48 mL/m^2, bases on *t*-test comparison.

Table 5 Correlation between LA function and age, systolic blood pressure, heart rate, LV function, LV structure, and LA size in patients with CA ($n = 124$)

Variables	Pearson's correlation (*P*-value)			
	LA reservoir function		LA conduit function	LA pump function
	Peak LS	Peak LSR	Early LSR	Late LSR
Age	-0.25 ($P = 0.01$)	-0.32 ($P = 0.0012$)	0.35 ($P = 0.0003$)	0.12 ($P = 0.24$)
Systolic blood pressure	0.09 ($P = 0.38$)	0.05 ($P = 0.64$)	-0.05 ($P = 0.67$)	-0.14 ($P = 0.20$)
Heart rate	-0.16 ($P = 0.10$)	0.02 ($P = 0.86$)	-0.15 ($P = 0.12$)	-0.04 ($P = 0.74$)
LV structure				
LVEDV/BSA	0.01 ($P = 0.92$)	-0.08 ($P = 0.42$)	-0.07 ($P = 0.50$)	-0.04 ($P = 0.67$)
LV mass index/BSA	-0.28 ($P < 0.0001$)	-0.26 ($P = 0.0077$)	0.08 ($P = 0.42$)	0.22 ($P = 0.0270$)
LV function				
LV GLS	-0.60 ($P < 0.0001$)	-0.54 ($P < 0.0001$)	0.30 ($P = 0.0020$)	0.54 ($P < 0.0001$)
LV ejection fraction	0.48 ($P < 0.0001$)	0.52 ($P < 0.0001$)	-0.27 ($P = 0.0066$)	-0.41 ($P < 0.0001$)
E wave	-0.16 ($P = 0.11$)	-0.06 ($P = 0.58$)	-0.01 ($P = 0.92$)	0.18 ($P = 0.08$)
A wave	0.57 ($P < 0.0001$)	0.55 ($P < 0.0001$)	-0.34 ($P = 0.0013$)	-0.69 ($P < 0.0001$)
E/E' (lateral)	-0.32 ($P = 0.0030$)	-0.25 ($P = 0.024$)	0.20 ($P = 0.06$)	0.26 ($P = 0.0183$)
LA structure				
LA width	-0.36 ($P = 0.0002$)	-0.38 ($P = 0.0001$)	0.41 ($P < 0.0001$)	0.31 ($P = 0.0017$)
LA volume index	-0.36 ($P = 0.0002$)	-0.36 ($P = 0.0002$)	0.30 ($P = 0.0025$)	0.31 ($P = 0.0021$)

LVEDV, left ventricular end-diastolic volume; BSA, body surface area; GLS, global longitudinal strain; E/E', mitral inflow to mitral relaxation velocity ratio.

Discussion

This is the first study that provides a systematic assessment of LA function in a large cohort of consecutive patients with the three main aetiologies of CA.

We showed that all 2D speckle-tracking derived LA phasic functions were severely impaired in CA and highly correlated with LV deformation. LA reservoir function (peak LS) was correlated with LVMI, LV GLS, LVEF, and diastolic measures and LA dimensions. In our cohort, ATTRwt seemed to show the worst profile of LA function. These findings support speckle-tracking imaging as a sensitive tool to assess LA function in CA and aim to gain further insights into the pathophysiology of LA dysfunction in CA.

Echocardiographically, LA function has been classically studied by means of LA size, phasic volumes, and emptying fraction. In particular, LA dimensions and volumes have been widely correlated with cardiovascular morbidity and mortality in various pathological conditions.[24,25] However, LA phasic volumes can be influenced by loading conditions. TDI-derived myocardial velocities provide a less load dependant measure of both LV systolic and diastolic function, where a' represents a marker of atrial function. However, TDI measures are angle-dependent and can be influenced by translation and tethering. On the other hand, strain analysis using speckle tracking is a direct measurement of intrinsic LA myocardial deformation, relatively independent of loading conditions and geometric assumptions[26,27] and with high feasibility and reproducibility.[28]

Previous studies have addressed LA function in CA. Modesto *et al.*[29] showed an impaired reservoir function in AL patients (peak LS and peak LSR) by colour Doppler myocardial imaging. De Gregorio *et al.*[30] showed an impairment in LA reservoir and pump function among patients with TTR-CA and hypertrophic cardiomyopathy (HCM) ($n = 16$ in each group), as compared to normal controls, but mainly in the former group, irrespective of LA volume and LV ejection fraction. Our results are consistent with such findings. Indeed, we showed that LA conduit and active functions were impaired in all the three aetiologies of CA (*Table 3*). However, when considering LA conduit function, while early LSR was lower in CA than in controls, LA passive emptying fraction did not differ significantly between CA and controls, suggesting that LA volume changes (conduit function) may be a compensatory mechanism when LA reservoir and pump function are impaired.

Worse LA strain was correlated with a greater impairment of LV systolic and diastolic function. This association suggests that amyloid infiltration progressively impairs both LV and LA function in parallel. LV longitudinal systolic dysfunction, which is typical of myocardial amyloid infiltration, may contribute to LA dysfunction because of the influence of downward motion of the mitral plane during ventricular systole, leading to reduced systolic expansion of the LA.[31]

Taken together, our findings support the combination of restrictive LV physiology with raised filling pressures (due to intramyocardial amyloid infiltration) and intrinsic LA failure (due to direct amyloid infiltration) as the main determinant of LA enlargement and dysfunction in CA[21,32] Indeed, in our population LA strain was highly correlated with LV GLS. In addition, a direct injury of LA walls was suggested by the impairment in all LA function phases (independently of LA size), including late LSR (which reflects the intrinsic active LA contraction), that were significantly worse in CA than similar age and gender matched healthy controls, even after adjustment for LA volume, LV systolic and diastolic function. This finding is supported by previous magnetic resonance studies showing a relatively high prevalence of late gadolinium enhancement throughout the LA walls of CA patients.[32] The relatively low prevalence of significant mitral

regurgitation in our population suggests that mitral valve disease is not a major factor responsible for LA dysfunction in our patients.[33]

Patients with ATTRwt seemed to show worse LA function parameters compared to the other aetiologies of CA, especially AL. It is well known that ATTRwt is a disease characterized by slowly progressive amyloid deposition.[1] Indeed patients with ATTRwt had longer disease duration (median 24.4 months) compared to those with AL (8.6 months) or ATTRm (15.4 months). We therefore anticipated more morphological and functional impairment of both LA and LV in ATTRwt. However, as already reported by our and other groups, the severity of heart failure and survival are much worse in AL amyloidosis compared to ATTRwt[2,8] with a median survival of approximately 6 months in untreated AL amyloidosis with heart failure and 6 years in ATTRwt.[2] It was out of scope of the present study to address the natural history and prognostic role of LA dysfunction among the different aetiologies of CA. However, it is likely that in ATTRwt, given the more chronic nature of amyloid deposition, compensatory mechanisms occur to counteract the effects of myocardial amyloid infiltration, including LV hypertrophy. On the contrary, in AL, an acute toxic effect exerted directly on cardiac myocytes[34] or a more rapid rate of amyloid infiltration may lead to LA dysfunction even in the absence of significant LA dilatation. Furthermore, other non-myocardial factors (including multi-organ involvement, autonomic dysfunction, or a direct microvascular infiltration) may play a critical role in the poor prognosis of AL amyloid subtype.[35]

Clinical implications

Although often ignored, the assessment of LA function in CA should be performed routinely in the clinical practice. Indeed, even in the absence of supraventricular arrhythmias such as atrial fibrillation or atrial flutter, patients with CA are predisposed to developing mural thrombi. In one large necropsy series, 26% of patients with cardiac amyloidosis were found to have intra-cardiac thrombi.[36] In another series, 42/156 (27%) CA patients undergoing transoesophageal echocardiography were diagnosed with intracardiac thrombi, with a higher frequency in AL vs. other aetiologies (35% vs. 18%), despite older age and a higher prevalence of atrial fibrillation in the non-AL group.[37,38] This phenomenon, which is generally due to atrial standstill derived from markedly increased LV diastolic pressures and intrinsic LA dysfunction, raises concerns regarding the appropriate use of anticoagulation therapy in CA. In this context, the study of LA function by means of standard and speckle tracking deformation imaging could represent a useful clinical tool to identify CA patients with higher thromboembolic risk in whom anticoagulation may be indicated beyond the standard risk scores (including CHADSVASC and CHA_2DS_2VASC)."

Limitations

Several limitations should be noted. This study included a large series of patients with the three main aetiologies of CA. However, the absolute number of patients within each aetiology is relatively small. To provide reference values of LA strain and SR, we selected healthy individuals as controls. However, we acknowledge that the number of age-matched healthy controls was small and we did not compare our findings with those of patients with similar degrees of LA enragement due to other cardiac diseases such as dilated or hypertrophy cardiomyopathy. This may limit our ability to distinguish between the effect of direct amyloid infiltration and more passive effects secondary to LV dysfunction in determining LA dysfunction. The overall advanced stage of the disease presented by CA patients in the present study precludes any possible insights into the earlier stages of CA, which will need a dedicated study. Finally, this study did not include any correlation with clinical outcomes, limiting the power to assess the predictive value of LA strain measurements.

Conclusions

In patients with CA, each phase of LA function assessed by 2D speckle-tracking echocardiography was severely impaired and highly correlated to left ventricular deformation but independent of LA size. The impairment of both passive and active LA function suggests a combination of both LV and intrinsic LA failure in the pathophysiology of LA dysfunction.

Despite the known different clinical courses, LA function was more impaired in ATTRwt compared to AL amyloidosis. This might indicate that in AL, given the more rapid progression of amyloid infiltration and the direct toxic effect exerted by circulating light chains on cardiac myocytes, cardiac dysfunction and heart failure may precede the overt morphological and functional left ventricular and atrial impairment, which seem to be more pronounced in ATTRwt due to a longer course of amyloid deposition.

Supplementary data

Supplementary data are available at *European Heart Journal—Cardiovascular Imaging* online.

Conflict of interest: None declared.

Funding

This work was partially supported by the grant from the Italian Ministry of Health—GR-2011-02352282 (C.C.Q.).

References

1. Falk RH. Diagnosis and management of the cardiac amyloidoses. *Circulation* 2005;**112**:2047–60.
2. Rapezzi C, Merlini G, Quarta CC, Riva L, Longhi S, Leone O *et al.* Systemic cardiac amyloidoses: disease profiles and clinical courses of the 3 main types. *Circulation* 2009;**120**:1203–12.
3. Merlini G, Bellotti V. Molecular mechanisms of amyloidosis. *N Engl J Med* 2003;**349**:583–96.
4. Quarta CC, Solomon SD, Uraizee I, Kruger J, Longhi S, Ferlito M *et al.* Left ventricular structure and function in transthyretin-related versus light-chain cardiac amyloidosis. *Circulation* 2014;**129**:1840–9.
5. Falk RH, Quarta CC. Echocardiography in cardiac amyloidosis. *Heart Fail Rev* 2015;**20**:125–31.
6. Mohty D, Pibarot P, Dumesnil JG, Darodes N, Lavergne D, Echahidi N *et al.* Left atrial size is an independent predictor of overall survival in patients with primary systemic amyloidosis. *Arch Cardiovasc Dis* 2011;**104**:611–8.
7. Kraigher-Krainer E, Shah AM, Gupta DK, Santos A, Claggett B, Pieske B *et al.* Impaired systolic function by strain imaging in heart failure with preserved ejection fraction. *J Am Coll Cardiol* 2014;**63**:447–56.
8. Ng B, Connors LH, Davidoff R, Skinner M, Falk RH. Senile systemic amyloidosis presenting with heart failure: a comparison with light chain-associated amyloidosis. *Arch Intern Med* 2005;**165**:1425–9.
9. Benson MD, Breall J, Cummings OW, Liepnieks JJ. Biochemical characterisation of amyloid by endomyocardial biopsy. *Amyloid* 2009;**16**:9–14.
10. Gertz MA, Comenzo R, Falk RH, Fermand JP, Hazenberg BP, Hawkins PN *et al.* Definition of organ involvement and treatment response in immunoglobulin light chain amyloidosis (AL): a consensus opinion from the 10th International Symposium on Amyloid and Amyloidosis, Tours, France, 18-22 April 2004. *Am J Hematol* 2005;**79**:319–28.

11. Rapezzi C, Quarta CC, Guidalotti PL, Longhi S, Pettinato C, Leone O *et al.* Usefulness and limitations of 99mTc-3,3-diphosphono-1,2-propanodicarboxylic acid scintigraphy in the aetiological diagnosis of amyloidotic cardiomyopathy. *Eur J Nucl Med Mol Imaging* 2011;**38**:470–8.
12. Bokhari S, Castano A, Pozniakoff T, Deslisle S, Latif F, Maurer MS. (99m)Tc-pyrophosphate scintigraphy for differentiating light-chain cardiac amyloidosis from the transthyretin-related familial and senile cardiac amyloidoses. *Circ Cardiovasc Imaging* 2013;**6**:195–201.
13. Lachmann HJ, Booth DR, Booth SE, Bybee A, Gilbertson JA, Gillmore JD *et al.* Misdiagnosis of hereditary amyloidosis as AL (primary) amyloidosis. *N Engl J Med* 2002;**346**:1786–91.
14. Palladini G, Perfetti V, Merlini G. Therapy and management of systemic AL (primary) amyloidosis. *Swiss Med Wkly* 2006;**136**:715–20.
15. Ferlini A, Fini S, Salvi F, Patrosso MC, Vezzoni P, Forabosco A. Molecular strategies in genetic diagnosis of transthyretin-related hereditary amyloidosis. *FASEB J* 1992;**6**:2864–6.
16. Westermark P, Sletten K, Johansson B, Cornwell GG 3rd. Fibril in senile systemic amyloidosis is derived from normal transthyretin. *Proc Natl Acad Sci U S A* 1990;**87**:2843–5.
17. Vrana JA, Gamez JD, Madden BJ, Theis JD, Bergen HR 3rd, Dogan A. Classification of amyloidosis by laser microdissection and mass spectrometry-based proteomic analysis in clinical biopsy specimens. *Blood* 2009;**114**:4957–9.
18. Lang RM, Bierig M, Devereux RB, Flachskampf FA, Foster E, Pellikka PA *et al.* Recommendations for chamber quantification: a report from the American Society of Echocardiography's Guidelines and Standards Committee and the Chamber Quantification Writing Group, developed in conjunction with the European Association of Echocardiography, a branch of the European Society of Cardiology. *J Am Soc Echocardiogr* 2005;**18**:1440–63.
19. Lang RM, Badano LP, Mor-Avi V, Afilalo J, Armstrong A, Ernande L *et al.* Recommendations for cardiac chamber quantification by echocardiography in adults: an update from the American Society of Echocardiography and the European Association of Cardiovascular Imaging. *Eur Heart J Cardiovasc Imaging* 2015;**16**:233–71.
20. Nagueh SF, Appleton CP, Gillebert TC, Marino PN, Oh JK, Smiseth OA *et al.* Recommendations for the evaluation of left ventricular diastolic function by echocardiography. *J Am Soc Echocardiogr* 2009;**22**:107–33.
21. Rossi A, Gheorghiade M, Triposkiadis F, Solomon SD, Pieske B, Butler J. Left atrium in heart failure with preserved ejection fraction: structure, function, and significance. *Circ Heart Fail* 2014;**7**:1042–9.
22. Cameli M, Lisi M, Mondillo S, Padeletti M, Ballo P, Tsioulpas C *et al.* Left atrial longitudinal strain by speckle tracking echocardiography correlates well with left ventricular filling pressures in patients with heart failure. *Cardiovasc Ultrasound* 2010;**8**:14.
23. Santos AB, Kraigher-Krainer E, Gupta DK, Claggett B, Zile MR, Pieske B *et al.* Impaired left atrial function in heart failure with preserved ejection fraction. *Eur J Heart Fail* 2014;**16**:1096–103.
24. Pritchett AM, Jacobsen SJ, Mahoney DW, Rodeheffer RJ, Bailey KR, Redfield MM. Left atrial volume as an index of left atrial size: a population-based study. *J Am Coll Cardiol* 2003;**41**:1036–43.
25. Moller JE, Hillis GS, Oh JK, Seward JB, Reeder GS, Wright RS *et al.* Left atrial volume: a powerful predictor of survival after acute myocardial infarction. *Circulation* 2003;**107**:2207–12.
26. Boyd AC, Richards DA, Marwick T, Thomas L. Atrial strain rate is a sensitive measure of alterations in atrial phasic function in healthy ageing. *Heart* 2011;**97**:1513–9.
27. Zhang Q, Yip GW, Yu CM. Approaching regional left atrial function by tissue Doppler velocity and strain imaging. *Europace* 2008;**10**(Suppl 3):iii62–9.
28. Cameli M, Caputo M, Mondillo S, Ballo P, Palmerini E, Lisi M *et al.* Feasibility and reference values of left atrial longitudinal strain imaging by two-dimensional speckle tracking. *Cardiovasc Ultrasound* 2009;**7**:6.
29. Modesto KM, Dispenzieri A, Cauduro SA, Lacy M, Khandheria BK, Pellikka PA *et al.* Left atrial myopathy in cardiac amyloidosis: implications of novel echocardiographic techniques. *Eur Heart J* 2005;**26**:173–9.
30. de Gregorio C, Dattilo G, Casale M, Terrizzi A, Donato R, Di Bella G. Left atrial morphology, size and function in patients with transthyretin cardiac amyloidosis and primary hypertrophic cardiomyopathy-comparative strain imaging study. *Circ J* 2016;**80**:1830–7.
31. Timek TA, Miller DC. Experimental and clinical assessment of mitral annular area and dynamics: what are we actually measuring? *Ann Thorac Surg* 2001;**72**:966–74.
32. Kwong RY, Heydari B, Abbasi S, Steel K, Al-Mallah M, Wu H *et al.* Characterization of cardiac amyloidosis by atrial late gadolinium enhancement using contrast-enhanced cardiac magnetic resonance imaging and correlation with left atrial conduit and contractile function. *Am J Cardiol* 2015;**116**:622–9.
33. Cappelli F, Baldasseroni S, Bergesio F, Perlini S, Salinaro F, Padeletti L *et al.* Echocardiographic and biohumoral characteristics in patients with AL and TTR amyloidosis at diagnosis. *Clin Cardiol* 2015;**38**:69–75.
34. Brenner DA, Jain M, Pimentel DR, Wang B, Connors LH, Skinner M *et al.* Human amyloidogenic light chains directly impair cardiomyocyte function through an increase in cellular oxidant stress. *Circ Res* 2004;**94**:1008–10.
35. Bernardi L, Passino C, Porta C, Anesi E, Palladini G, Merlini G. Widespread cardiovascular autonomic dysfunction in primary amyloidosis: does spontaneous hyperventilation have a compensatory role against postural hypotension? *Heart* 2002;**88**:615–21.
36. Roberts WC, Waller BF. Cardiac amyloidosis causing cardiac dysfunction: analysis of 54 necropsy patients. *Am J Cardiol* 1983;**52**:137–46.
37. Feng D, Edwards WD, Oh JK, Chandrasekaran K, Grogan M, Martinez MW *et al.* Intracardiac thrombosis and embolism in patients with cardiac amyloidosis. *Circulation* 2007;**116**:2420–6.
38. Feng D, Syed IS, Martinez M, Oh JK, Jaffe AS, Grogan M *et al.* Intracardiac thrombosis and anticoagulation therapy in cardiac amyloidosis. *Circulation* 2009;**119**:2490–7.